

Analytical Modeling of Magnetically Saturated Inductance by Lambert W Function

Hilmi Gurleyen^{1*} and Erkan Mese²

¹Department of Electrical Engineering, Yildiz Technical University, Istanbul 34220, Turkey

²Department of Electrical and Electronics Engineering, Ege University, Izmir 35100, Turkey

(Received 27 April 2017, Received in final form 22 August 2017, Accepted 25 August 2017)

Inductance is one of the most important components in order to make energy conversion in the power converters. The dynamics of power converter are affected by inductance. Therefore, in order to obtain accurate power converter dynamic model, one needs to have accurate inductance model. An inductance value is not always constant as it depends on current. Especially in the saturation region, inductance value decreases when current increases. On the other hand, exact eddy current and hysteresis losses estimation can be obtained with an accurate inductance model. This paper proposes an improved analytical inductance model that considers nonlinear B-H curve of a core material. A nonlinear B-H function is fitted using the Matlab Curve Fitting Toolbox. This function includes magnetic flux density (B) against magnetic field strength (H) variation in the both linear and saturation regions. The magnetic circuit model is obtained using a lumped parameter method and the Lambert W function is used to solve the equation which includes nonlinear core reluctance. In conclusion, a nonlinear analytical inductance model is proposed.

Keywords : nonlinear magnetic circuit model, nonlinear analytical inductance model, saturation

1. Introduction

Inductance plays an important role in DC-DC converters' energy conversion process. Inductance affects most of the DC-DC converter parameters like the current ripple, current working mode etc. [1]. Unfortunately, the inductance value is not always constant due to the nonlinear magnetization (B-H) behavior of the core. Especially, in the saturation region, the inductance value decreases dramatically. Although many studies exist regarding the power converter models which have a linear inductance model, inductance of power converters is nonlinear [2]. Nonlinear inductance affects the performance of current controllers for the power converters [3]. The effect of nonlinear inductance for the model predictive control methods is illustrated in [4, 5]. Particularly, in order to improve the performance for the model predictive control, nonlinear inductance effect should be considered.

Core losses are another important aspect in designing any power converter. Magnetic flux density plays important

role to predict eddy and hysteresis losses. These losses are obtained using Steinmetz equation [6]. A dynamic core loss model is presented in [7] using Finite Element Analysis (FEA). Saturation and thermal effect are shown in [8]. The Steinmetz equation for air gapped magnetics cores is illustrated in [9]. Proper core loss prediction with a reasonable computational effort always requires flux density calculation which becomes cumbersome in a saturated core. Hence simplifying calculation tools for the flux density would be quite valuable for someone desiring fast core loss prediction.

There are several studies which investigate inductance saturation in the literature. In [10, 11], a nonlinear transformer is modeled. Some of the investigations attempt to model nonlinear inductance by FEA [12-14]. Also, analytical nonlinear modeling approaches are shown in [15, 16]. In some applications, inductance saturation is unavoidable. For instance, DC-DC power converters used in low voltage and high current applications like electrical vehicles [17, 18] experience saturation. Inserting air gap in these applications is commonly used remedy to manage saturation. On the other hand, the behavior of a saturated inductor without air gap can be predicted by analytical solution in a simpler fashion by using B-H curve functions.

©The Korean Magnetism Society. All rights reserved.

*Corresponding author: Tel: +905445404816

Fax: +90212 383 58 58, e-mail: hilmigurleyen@gmail.com

Air gap changes magnetic behavior of the complete inductor and conventional analytical methods are no longer accurate.

In this study, a saturated inductance with an air gap is analytically modeled by using lumped parameter method. Firstly, the nonlinear B-H curve is presented by a simple mathematical function. After that, the magnetic equivalent equation is obtained by taking into account the nonlinear core reluctance. Air gap reluctance is considered as constant. Iterative methods may be used to solve the nonlinear equation. Novelty proposed in this paper is that Lambert W function is used to solve the nonlinear magnetic equivalent circuit. As a conclusion, an exact solution is obtained and system parameters like inductance value, flux, flux density, magnetic field strength can also be calculated. These parameters may then be used in both control and power loss calculation. Nonlinear inductance model is used in a buck converter to demonstrate the accuracy of the proposed method. Since Lambert W function is available in the Matlab, proposed model is simulated using Matlab. Then the results are compared with conventional model simulations which are based on linear inductance model. After that, the proposed model is validated by experimental results.

2. Mathematical Model for B-H Curve

Magnetization behavior of a core is important parameter during inductance design process. There are many mathematical expressions to obtain B versus H relation of cores [19]. In this paper, (1) is used for this purpose.

$$B = c_1(1 - \exp(c_2H)) + c_3H \quad (1)$$

Here, c_1 , c_2 and c_3 are coefficients and depend on the core material. The advantage of this expression is its simplicity, but the disadvantage is the error introduced in the saturation region. In particular, when the B-H curve is sharp [20]. c_1 , c_2 and c_3 are determined by the Matlab Curve Fitting Toolbox. Figure 1 shows the curve fitted B-H curve along with the manufacturer data. Here, Kool M μ E core's magnetization data is used [21]. Figure 2 shows error between manufacturer data and fitted curve. At the beginning, there is a large error because of the fact that Eq. (1) does not consider remanence. Figure 1 shows very large operation range for the inductance which spans both linear and highly saturation regions. Although the fitted curve covers all of the operation regions, its estimation performance is low when the magnetic field strength is low. Figure 2 shows peak error is about 9.5 %. If the system works around the saturation, the error is

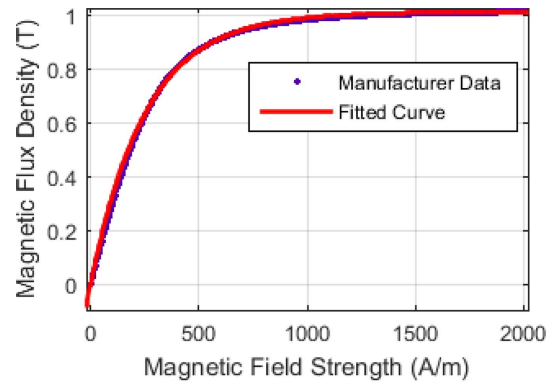


Fig. 1. (Color online) Manufacturer magnetization data and Matlab curve fitting result.

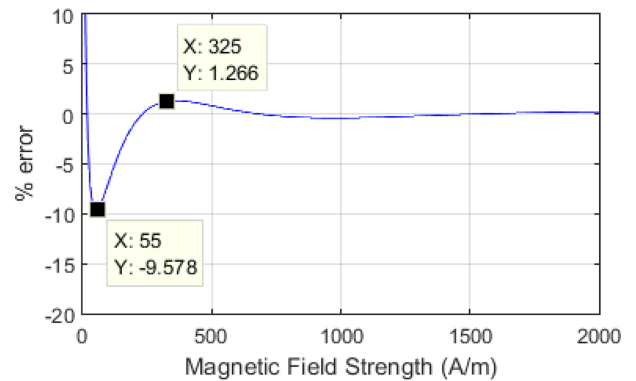


Fig. 2. (Color online) Error between manufacturer data and fitted curve.

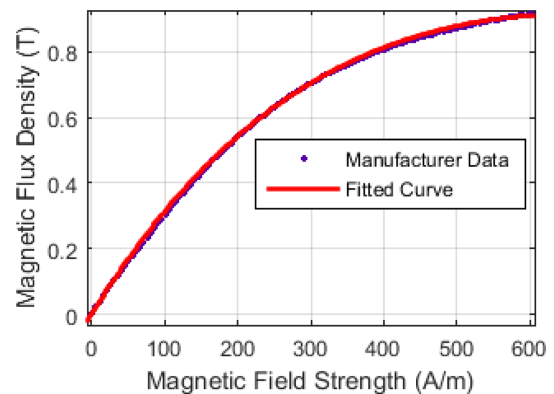


Fig. 3. (Color online) Manufacturer magnetization data and Matlab curve fitting result in the linear region.

about 0.3 %. After this observation instead of covering all operation area, linear region and low saturation region is considered in effort to obtain more accurate curve fitting. Figure 3 and Fig. 4 illustrate the curve fitting performance for limited range of data. Peak error decreases to 2.5 % except for remanence.

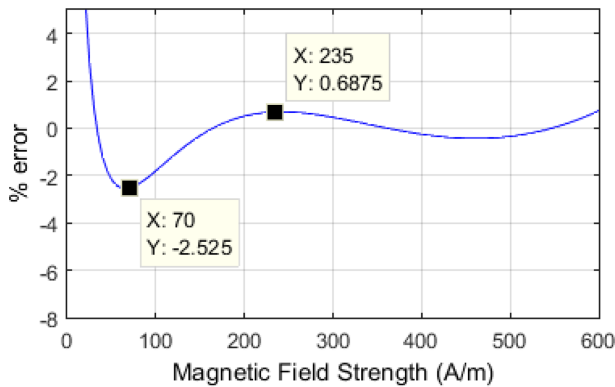


Fig. 4. (Color online) Error between manufacturer data and fitted curve in the linear region.

3. Nonlinear Inductance Model

In this section, a nonlinear magnetic circuit is obtained using lumped parameter method. Numerical method like Newton Raphson is used to solve the nonlinear equation. Such methods have disadvantages of error in the solution and computational burden due to its iterative nature. These are common issues from which other numerical techniques also suffer. Lambert W function is proposed in this paper in order to solve the nonlinear equation explicitly so that error and as well as solution times are reduced. Lambert W function is an inverse function of Eq. (2). ω is unknown and x is known parameters in Eq. (2). In order to obtain ω , Lambert W is used in Eq. (3), W , symbolize Lambert W function, in Eq. (3). Lambert W function can be used in case of the unknown parameter is both product and power of exponential as shown in Eq. (2). It is a predefined function in mathematical calculation programs such that; Matlab, Maple, etc. It is used different type of engineering applications [22].

$$\omega \exp^{\omega} = x \tag{2}$$

$$\omega = W(x) \tag{3}$$

Figure 5 shows structure of the inductance. Firstly, equations should be transformed from B-H form to flux-MMF form in order to create magnetic equivalent circuit. Table 1 shows units of magnetic properties which are used in the following equations. There is a relationship between magnetic field strength and magneto motive force. For that, H transforms into MMF using flux path according to Ampere's Law. Therefore Eq. (6) is obtained from Eq. (4). Flux can be obtained from products of B and core cross sectional area A. Figure 6 shows magnetic equivalent circuit. In this circuit, air gap reluctance is linear element whereas core reluctance is nonlinear. Air

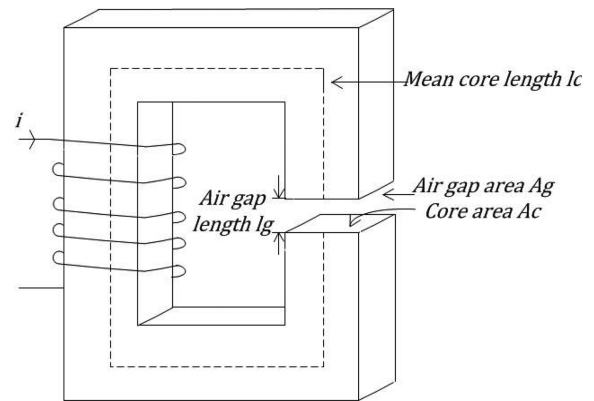


Fig. 5. Structure of inductance with air gap.

Table 1. Units for magnetic properties.

Symbol	Quantity	SI Units
Φ	Magnetic flux	Wb
B	Magnetic flux density	T or Wb/m ²
H_c	Magnetic field strength in the core	A/m
H_g	Magnetic field strength in the air gap	A/m
MMF	Magneto motive force	A.Turns
I	Current	A
N	Number of turns	Turns
R_g	Air gap reluctance	A/Wb
R_c	Core reluctance	A/Wb
l_c	Mean core length	m
l_g	Air gap length	m
A	Core cross sectional area	m ²
V	Magneto motor force	A.turns
μ	Permeability	Wb/(A.m)

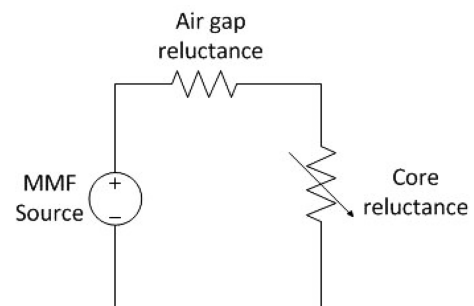


Fig. 6. Magnetic equivalent circuit.

gap area and core cross sectional area are assumed to be same. This implies that the fringing effect is excluded in the model under consideration.

If magnetic permeability is known in a magnetic system, finding a solution is simple for a particular operating point of Eq. (6). Unfortunately, magnetic permeability versus magnetic field strength relation is nonlinear. Therefore, the solution becomes challenging in Eq. (6) when the core

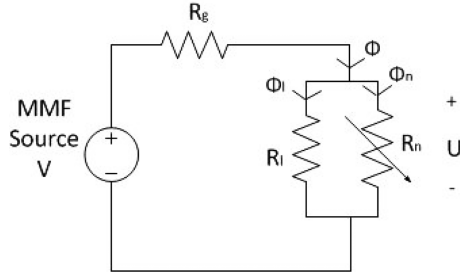


Fig. 7. Magnetic equivalent circuit in which core reluctance is separated.

operates in a wide range of magnetic field. In order to consider nonlinear B-H relationship, Eq. (1) is used and rewritten in Eq. (7) using magnetic flux and MMF instead of magnetic flux density and magnetic field strength, respectively. After that Eq. (11) is obtained using Eq. (8), (9) and (10). Here U represents MMF of the core. In a magnetic system, core geometry and core's B-H curve affect its magnetic performance. Both geometric dimensions and B-H curve are considered in Eq. (11) which forms the basis for the proposed model. It can be seen that Eq. (11) has a nonlinear part and a linear part. Hence Eq. (11) is divided into two part as being nonlinear Eq. (12) and linear Eq. (13). In this case, a new magnetic equivalent circuit is obtained in Fig. 7. In this circuit, \$R_g\$ and \$R_l\$ are linear and \$R_n\$ is nonlinear reluctances.

$$H_c l_c + H_g l_g = NI \tag{4}$$

$$NI = V \tag{5}$$

$$V = R_g \phi + R_c(\phi)\phi \tag{6}$$

$$\frac{\phi}{A} = c_1 \left(1 - \exp\left(-c_2 \frac{U}{l_c}\right) \right) + c_3 \frac{U}{l_c} \tag{7}$$

$$a_1 = A c_1 \tag{8}$$

$$a_2 = \frac{c_2}{l_c} \tag{9}$$

$$a_3 = \frac{A c_3}{l_c} \tag{10}$$

$$\phi = a_1(1 - \exp(a_2 U)) + a_3 U \tag{11}$$

$$\phi_n = a_1(1 - \exp(a_2 U)) \tag{12}$$

$$\phi_l = a_3 U \tag{13}$$

$$\phi = a_1(1 - \exp(a_2 U)) + a_3 U = \frac{V - U}{R_g} \tag{14}$$

$$\phi_n = \frac{V - U - R_g a_3 U}{R_g} \tag{15}$$

$$U = \frac{V - R_g \phi_n}{1 + R_g a_3} \tag{16}$$

$$\omega = \frac{a_2 R_g}{1 + R_g a_3} (-a_1 + \phi_n) \tag{17}$$

In order to utilize in Lambert function, let's define a new variable as follow,

$$\omega \exp(\omega) = \frac{a_2 R_g}{1 + R_g a_3} (-a_1 + a_1 - a_1 \exp(a_2 U)) \exp\left(\frac{a_2 R_g}{1 + R_g a_3} (-a_1 + \phi_n)\right) \tag{18}$$

$$\omega \exp(\omega) = \frac{a_2 R_g}{1 + R_g a_3} \left[-a_1 \exp\left(\frac{a_2 V}{1 + R_g a_3}\right) \exp\left(-\frac{a_2 R_g \phi_n}{1 + R_g a_3}\right) \right] \exp\left(-\frac{a_1 a_2 R_g}{1 + R_g a_3}\right) \exp\left(\frac{a_2 \phi_n R_g}{1 + R_g a_3}\right) \tag{19}$$

$$\omega \exp(\omega) = \frac{a_2 R_g}{1 + R_g a_3} \left(-a_1 \exp\left(\frac{a_2 (V - a_1 R_g)}{1 + R_g a_3}\right) \right) \tag{20}$$

$$\omega = W\left(\frac{a_2 R_g}{1 + R_g a_3} \left[-a_1 \exp\left(\frac{a_2 (V - a_1 R_g)}{1 + R_g a_3}\right) \right]\right) \tag{21}$$

$$\phi_n = \frac{\omega(1 + R_g a_3)}{a_2 R_g} + a_1 \tag{22}$$

$$U = \frac{1}{a_2} \ln\left(\frac{a_1 - \phi_n}{a_1}\right) \tag{23}$$

$$L = \frac{N \phi}{I} \tag{24}$$

Equation (14) is written by considering MMF balance in a series magnetic circuit. In this equation linear part of the flux is written to the right side. Nonlinear part of the flux is defined in Eq. (15). After that, \$\omega\$ is used for variable transformation as given in Eq. (17) in order to obtain a suitable equation for Lambert W function.

Equation (2) and (3) defines Lambert W function. Eq. (17) is plugged into Eq. (2) and Eq. (18) is obtained. Equation (15) and (16) is substituted in Eq. (18) as replacement of MMF and nonlinear flux. This operation yields Eq. (19). Equation (19) is simplified, Eq. (20) is obtained. Objective of this calculation is to eliminate variable terms in equation. It is clearly seen in Eq. (20) all

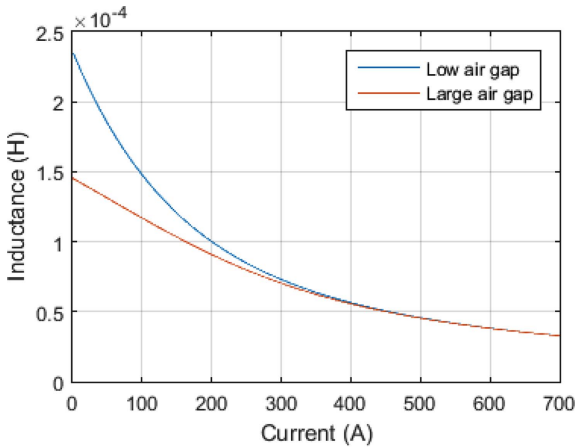


Fig. 8. (Color online) Inductance value against current.

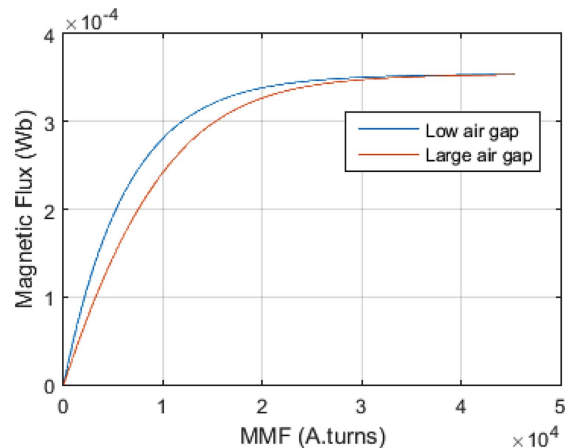


Fig. 9. (Color online) MMF-flux graphic.

of variable terms like U , Φ , Φ_n and Φ_l are disappeared. Equation is ready to apply Lambert W function. ω is found in Eq. (21) and thus, nonlinear part of flux is calculated using Eq. (22). After that MMF of the core is obtained in Eq. (23). After MMF is calculated, flux is found with Eq. (14). Finally, all of the variables are solved in the nonlinear magnetic circuit.

Air gap length affects inductance value of the magnetic system inversely. So, magnetic behavior of the magnetic system is dependent on air gap, too. Proposed method considers this relationship. Figure 8 shows that inductance value changes against magnetization current. In this figure

there are two different inductances which have identical dimensions and core material but different air gap. Inductance values are calculated using equations which mentioned above. Figure 9 illustrates flux versus MMF relation to demonstrate the effect of the air gap. In this figure MMF is total MMF which is provided by external source. Both of these figures shows that proposed model can consider air gap length and use it in calculations. Air gap length is defined as 0.01 mm for short air gap distance and 5 mm for long one in order to see the proposed method's performance on the inductance and flux linkage estimation for various air gap values.

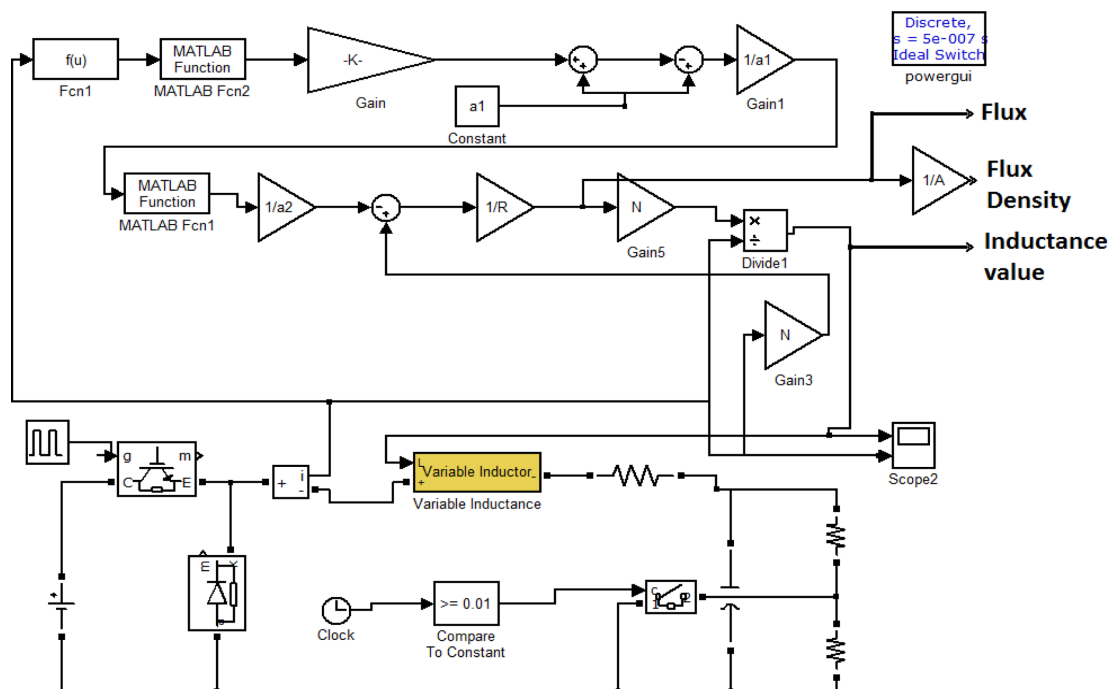


Fig. 10. (Color online) Buck converter Matlab/Simulink simulation with proposed inductance model.

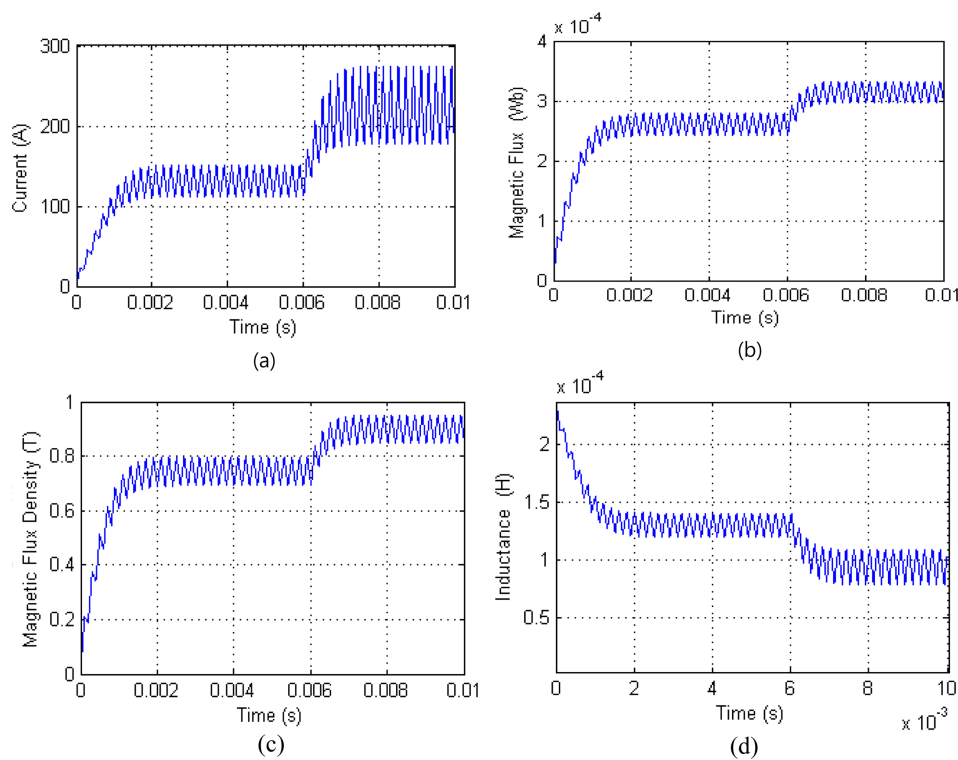


Fig. 11. (Color online) Buck converter Matlab/Simulink simulation with proposed inductance model.

4. Simulation Results

The dynamic simulation is very important during power converter design. Proposed model can be used in a dynamic simulation. This model gives information about system variables like current, flux, flux density and inductance. Current is very important to select power switch and diode. Also magnetic flux density is important to predict core loss. Inductance affects system dynamics and it is important to consider in the model predictive control. Proposed inductance model is simulated in a DC-DC buck converter using Matlab/Simulink as shown in Fig. 10. Figure 11(a) shows inductance current. In this simulation, load changes at 0.006 s. Figure 11(b) and Fig. 11(c) show magnetic flux and magnetic flux density, respectively.

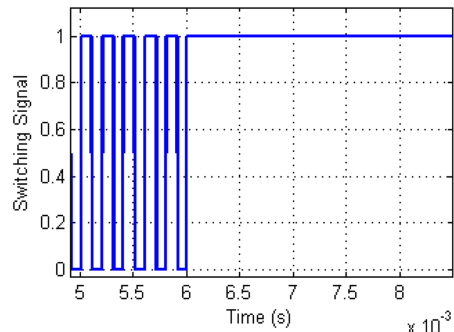
Figure 11(d) shows the variation of inductance value. It is obviously seen from this figure that when current increase, inductance value decreases and current ripple increases. Depending on the inductance current, magnetic flux density increases, too. Figure 12 shows that after the 0.006 s signal switch is permanently on. In this simulation, proposed model and standard linear inductance model is compared. After the switch turns on, current increases with much higher rate in the proposed model, which considers the saturation. Inductance value decreases dramatically after the saturation starts. Therefore, current

ripple increases. In contrary, linear model does not consider saturation. The difference between proposed and linear model can be seen in Fig. 12. This model also can be used to determine saturation current of inductance.

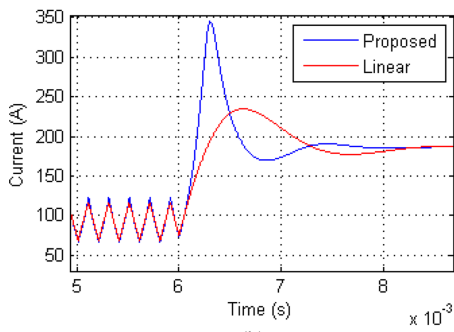
5. Experimental Results

A DC-DC buck converter has been built in order to validate proposed method experimentally. Figure 13 shows schematic diagram and Fig. 14 shows the photo of the experimental system. Kool M μ 00K55228E026 from Magnetics Inc. is used as an inductance core. The parameters are as follows: path length is 246 mm, cross section area is 350 mm². The number of turns is 65. Also, air gap length is 0.1 mm.

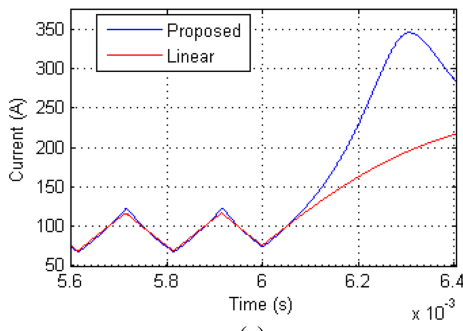
During the test, load was changed to observe inductance variation against current variation. Input voltage was adjusted by the auto-transformer. Single-phase full wave diode rectifier is used to transform AC to DC. In order to compare experimental results and simulation results inductance voltage levels are kept constant. Test duration was kept short to prevent damage to circuit. Figure 15 shows inductance voltage waveforms obtained in experimental and simulation studies. Voltage is not constant during positive cycle in the experimental result because there is a voltage ripple in the rectifier part of circuit.



(a)



(b)



(c)

Fig. 12. (Color online) (a) Switching signal (b) Inductance current (c) Zoomed inductance current.

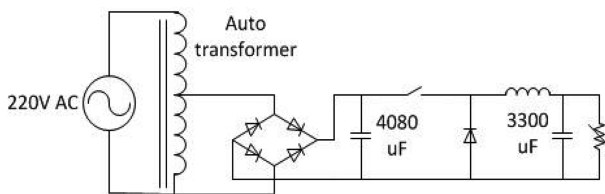


Fig. 13. Buck converter schematic diagram.

Current ripple is related with the inductance value and it is a good indicator of the inductance variation. Performance validation of the proposed model is performed by current ripple waveform comparison. In order to get a legitimate comparison between experimental and simulation results, inductance voltage waveforms are maintained at the same shape and level. According to the Fig. 16(a)

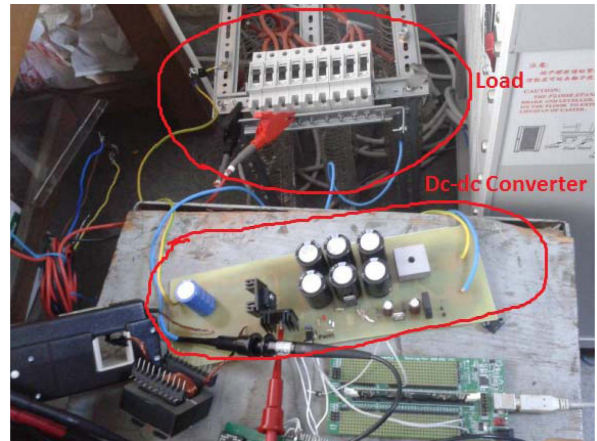


Fig. 14. (Color online) Buck converter test system photo.

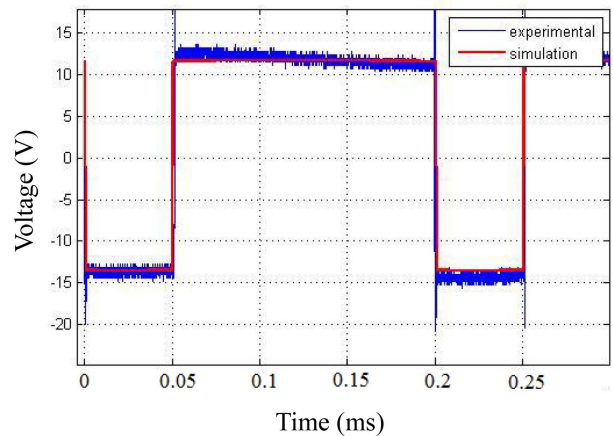


Fig. 15. (Color online) Inductance voltages during simulation and experiment.

inductance current of experimental circuit, linear (inductance value is constant) and proposed models are very close. However, Fig. 16(b) illustrates little difference between proposed and linear model and difference is largest in Fig. 16(c). On the other hand, experimental and proposed model current waveforms are very close. Current ripple is dependent on inductance value and figures show that inductance is varying as the current magnitude increases. It is clearly visible that proposed model can track inductance variation occurring at high current. Nonlinear nature of the core's B-H curve is taken into account by the proposed method and other secondary effects such as resistance variation, fringing effect and leakage inductance are neglected. However little difference between experimental current illustrated in Fig. 16(c) shows that magnetic saturation is dominant among the other reasons causing deviation. Hence the proposed model is performing well in catching up the experimental current waveforms with a higher fidelity.

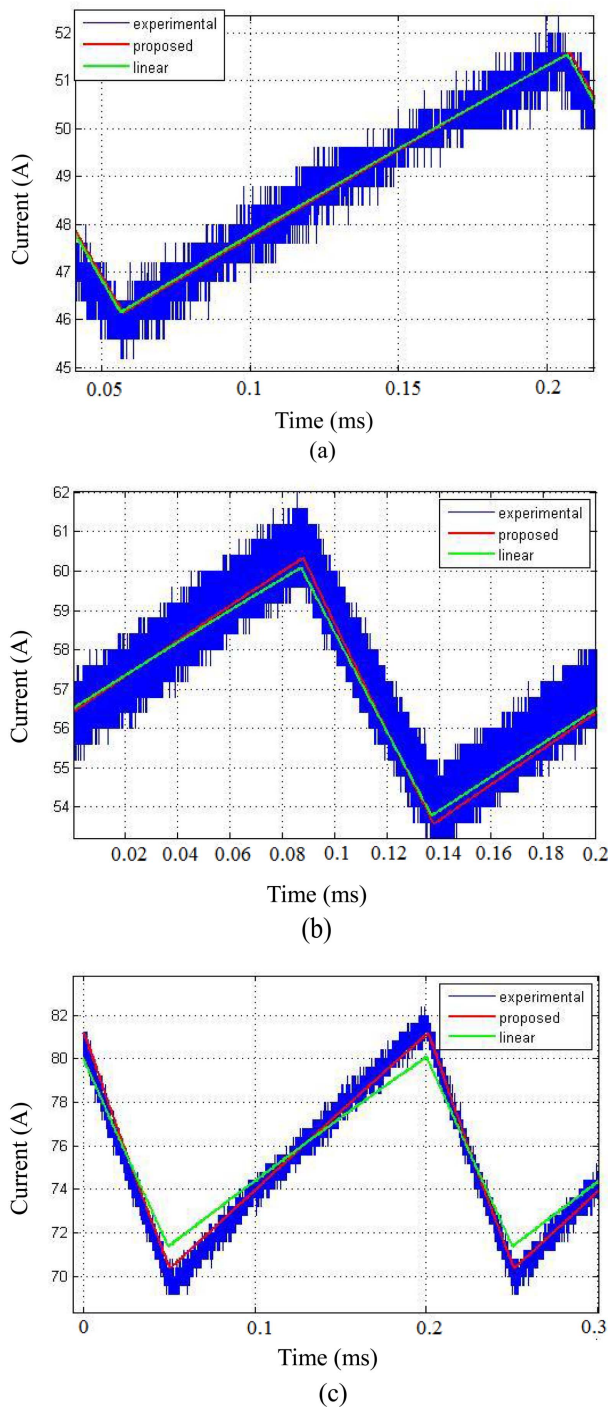


Fig. 16. (Color online) Inductance currents of experimental circuit, proposed and linear model.

6. Conclusion

A new analytical model has been proposed in order to calculate inductance value and magnetic flux density accurately considering the nonlinear behavior of inductance core. Lumped parameter method is used to obtain

magnetic equivalent circuit and core reluctance is defined as a nonlinear element. Lambert W function is used to solve the equation which includes nonlinear reluctance. After that, the proposed model is simulated using Matlab/Simulink and compared with experimental results. Ability to simulate proposed model in the dynamic simulation environment is the superiority of this model. The study shows that by taking into account nonlinearity of core's B-H curve very close matching between the model and experimental waveforms has been achieved. This model can eventually improve control performance of DC-DC converters which use model predictive control algorithm. Also proposed model can predict magnetic flux density accurately, this can be used to estimate core losses. On the other hand, B-H curve is dependent on temperature. c_1 , c_2 and c_3 coefficients can be determined by considering such temperature dependence. Hence the proposed model may be expanded to include thermal behaviors.

References

- [1] M. H. Rashid, Power Electronics Handbook, 2nd ed., Ed. New York: Academic (2007) pp. 245-255.
- [2] H. E. Fadil, F. Giri, O. El Magueri, and F. Z. Chaoui, Control Engineering Practice (2009).
- [3] R. A. Mastromauro, M. Liserre, and A. Dell'Aquila, IEEE Trans. Ind. Electron. **55**, 5 (2008).
- [4] S. Mariethoz, A. G. Beccuti, G. Papafotiou, and M. Morari, IEEE Appl. Power Electron. Conf. Expo. (2008).
- [5] S. Mariethoz, M. Hercegy, and M. Kvasnica, Control and Modelling for Power Elec., Conf. (2008).
- [6] C. P. Steinmetz, Trans. AIEE, **9**, 3 (1892).
- [7] D. Lin, P. Zhou, W. N. Fu, Z. Badics, and Z. J. Cendes, IEEE Trans. Magn. **40**, 2 (2004).
- [8] J. Y. Alsawalhi and S. D. Sudhoff, IEEE Trans. Magn. **49**, 11 (2013).
- [9] A. Ayachit and M. K. Kazimierczuk, IEEE Magn. Lett. **7**, 1 (2016).
- [10] J. D. Greene and C. A. Gross, IEEE Trans. Ind. Appl. **24**, 3 (1988).
- [11] T. C. Monteiro, F. O. Martinz, L. Matakas, and W. Komatsu, IEEE Trans. Ind. Appl. **48**, 3 (2012).
- [12] R. A. Salas and J. Pleite, IEEE Trans. Magn. **49**, 7 (2013).
- [13] R. A. Salas and J. Pleite, IEEE Trans. Magn. **47**, 10 (2011).
- [14] A. Salas, J. Pleite, E. Olías, and A. Barrado, IEEE Trans. Magn. **44**, 1891 (2008).
- [15] G. D. Capua and N. Femia, IEEE Trans. Power Electron. **31**, 3 (2016).
- [16] A. V. Radun, IEEE Trans. Magn. **50**, 5 (2014).
- [17] B.-G. You, S.-W. Lee, G.-B. Choi, D.-W. Yoo, and B. Lee, Proc. IEEE ICPE ECCE (2011).
- [18] B.-G. You, J.-S. Kim, B.-K. Lee, G.-B. Choi, and D.-W.

- Yoo, Proc. IEEE Vehicle Power Propulsion Conf. (2011).
- [19] Q. Tang, Z. Wang, P. I. Anderson, P. Jarman, and A. J. Moses, IEEE Trans. Magn. **51**, 5 (2015).
- [20] D. A. Torrey and J. H. Lang, Proc. Inst. Elect. Eng. B, **137**, 315 (1990).
- [21] Magnetics Inc. (2015) “2015 Magnetics Powder Core Catalog”, [Online]. <https://www.mag-inc.com/design/technical-documents/powder-core-documents>
- [22] R. M. Corless, G. H. Gonnet, D. E. G. Hare, D. J. Jeffrey, and D. E. Knuth Advances in Computational Mathematics **5**, 4 (1996).